



## Thermal properties of soil in the Murrumbidgee River Catchment (Australia)



B. Usowicz<sup>a</sup>, M.I. Łukowski<sup>a,\*</sup>, C. Rüdiger<sup>b</sup>, J.P. Walker<sup>b</sup>, W. Marczewski<sup>c</sup>

<sup>a</sup> Institute of Agrophysics, Polish Academy of Sciences, Doświadczalna 4, 20-290 Lublin, Poland

<sup>b</sup> Department of Civil Engineering, Monash University, Clayton, Victoria 3800, Australia

<sup>c</sup> Space Research Centre, Polish Academy of Sciences, Bartycka 18A, 00-716 Warsaw, Poland

### ARTICLE INFO

#### Article history:

Received 25 April 2017

Received in revised form 7 August 2017

Accepted 8 August 2017

#### Keywords:

Bulk density

Water content

Temperature

Thermal conductivity

Heat capacity

Thermal diffusivity

Soil

### ABSTRACT

This paper presents analyses of topsoil thermal conductivity, heat capacity, thermal diffusivity, water content, and bulk density obtained during the Australian Airborne Cal/Val Experiment for SMOS. The aim of the study presented here is to identify the structure and variability of the spatial distribution of soil properties and their mutual dependencies. Knowledge of the spatial distribution of soil bulk density and water content is essential to develop precise agronomic practices to manage the thermal properties of the soil and the quality and efficiency of cultivated plants. Thermal properties of soils were obtained from *in situ* measurements and modelled using the Usowicz statistical-physical model which is based on simple physical soil properties. Two soil water content measurement methods (gravimetric and dielectric) and two soil granulometry classification systems (USDA and Australian) were used to find the most effective approach. It is shown that: (i) quartz and water content and the bulk density of soil are the main factors affecting the thermal properties of the soil; (ii) the spatial distribution of conductivity and heat capacity is governed by the soil water content distribution, while the thermal diffusivity near its maximum is mainly driven by the spatial distribution of the bulk density; and (iii) soil thermal properties were estimated more accurately from the Australian soil granulometry than the USDA classification. The results not only improved the scarce information about thermal properties of Australian soils, but allow to estimate the soil thermal properties across large scales from the physical properties of the soil (based on existing databases) and the current soil water content (from satellite and/or *in situ* measurements).

© 2017 Elsevier Ltd. All rights reserved.

### 1. Introduction

Soil thermal properties are one of the main factors determining mass and energy exchange processes taking place on Earth. Determination of soil thermal properties and spatial variability is therefore an important factor in understanding these processes across all scales. The thermal conditions at the field scale have a significant impact on local climate and growth and development of plants. The energy exchange on the land surface is described by the surface energy balance equation, consisting of four components [1]: soil heat flux, latent heat flux, sensible heat flux and the net radiation. While the latter three are quite well described and relatively straightforward to measure *in situ* or by remote sensing methods [2], soil heat flux needs to be investigated with more attention. Knowledge about soil thermal properties has

significant practical consequences. It can be utilized for the evaluation of optimum conditions for plants and for the control of thermal-moisture regimes of soil in the field or in a greenhouse.

The thermal regime and heat flux in the soil is dependent on the amount of energy reaching the surface, heat accumulated in the soil, and the soil thermal properties. The amount of heat exchanged in the soil is also affected by general climatic conditions, topography, time of day, weather, and the characteristics of the active surface (e.g. vegetation coverage, soil type) where transformation of radiation and energy exchange occur. Incoming energy and accumulated heat is changing rapidly and randomly partly due to the nature of wind and cloud cover. Conversely, thermal properties of the soil depend on well-defined physical properties and the soil state, and may be considered as semi-stable [3]. However, information on thermal properties of soils is very limited or does not exist at all.

Local thermal properties of the soil are determined by its mineralogical composition, particle size distribution, organic matter

\* Corresponding author.

E-mail address: [m.lukowski@ipan.lublin.pl](mailto:m.lukowski@ipan.lublin.pl) (M.I. Łukowski).

content, density of the solid phase and the bulk density of the soil, water content and temperature [4–19]. The first five properties are temporarily stable or semi-stable, while soil water content and temperature are spatially and temporarily variable. Water content and temperature of the soil, as well as meteorological variables, can be measured by a range of monitoring systems (towers, aircrafts or satellites) [20–22]. At small and medium spatial scales they may be measured *in situ* by hand-held devices [23]. The bulk density of the soil is generally determined by the gravimetric method, through extraction of soil samples. In porous mediums such as soil, it is difficult to remotely measure the thermal properties, and even more difficult to determine their space- and time distribution over large areas [22,23]. Therefore, it is important to develop methods for determining the thermal properties of the soil via other easily measurable physical soil properties such as texture or density [18].

This study uses the statistical-physical model of thermal conductivity developed by Usovicz [18] to determine the thermal properties of the soil in the Murrumbidgee River catchment in south-eastern Australia. To determine the thermal diffusivity and heat capacity of the soil, the well-known de Vries empirical formulas [7] were used. Thermal properties were measured *in situ* at selected points during the AACES-1 field campaign [26] and compared with model predictions.

Estimation of the quartz and other minerals content was based on Australian and USDA classifications of the soil particle size distributions [24]. Examination of the spatial variation of the thermal conductivity, heat capacity and thermal diffusivity of the surface layer of the soil was conducted under a variety of land covers, with consideration of the water content, density and temperature of the soil.

## 2. Study site and methods

Measurements of soil water content, bulk density, temperature, soil thermal conductivity, and meteorological data analyzed in this study were collected across the Murrumbidgee River catchment in Australia (Fig. 1) during the first Australian Airborne Cal/Val Experiment for SMOS (AACES-1) [26].

The campaign was carried out during the Australian summer, from 18 January to 21 February 2010, on soils derived from a variety of rocks (Fig. 2a) resulting in diverse texture (Fig. 2b).

Soils across the western part of the catchment are dominantly clay, clay loam and loam derived from sedimentary rocks. The lithology of the eastern part of the catchment is more complicated. There are elongated, longitudinally-arranged areas of granites, felsic and mafic volcanics, sedimentary rocks and some serpentinites. Loamy soils were formed on these bedrocks that gradually turn into sandy loams towards the eastern part of the catchment. The south-eastern part of the Murrumbidgee River catchment is a mixture of loam, sandy loam and clay loam, formed due to erosion processes in the Australian alpine region.

Measurements of soil water content, temperature and electrical conductivity in the surface layer of soil were carried out using the Hydra Probe II instrument (which is a frequency domain reflectometer, part of the HDAS – Hydraprobe Data Acquisition System [27]) with simultaneous measurements of the current location by GPS. Collocated with a number of those measurements, soil thermal conductivities were determined using the Decagon KD2 Pro meter attached to the SH-1 dual-needle sensor. In close proximity to the *in situ* water content measurements, soil samples were taken in 180 cm<sup>3</sup> cylinders for further examination in laboratory. During each *in situ* measurement, the KD2 and Hydra Probe needles were stuck approximately down to 4–6 cm into soil, which is similar to the cylinder penetration depth, so it was assumed that thermal properties, water contents and samples were taken from the same soil layer. In laboratory soil bulk densities and gravimetric water contents were obtained using standard method requiring weight of wet sample and after 24 h oven-drying in 105 °C. The same soil samples were examined to determine soil particle size distribution using the laser and areometric methods [28]. Solid phase density (specific gravity) was measured by a helium pycnometer (ULTRA-PYC 1200e, Quantachrome Instruments) according to the standard procedure.

### 2.1. Thermal properties and the statistical-physical model

Soil thermal property estimation was performed by using empirical relationships and the Usovicz's statistical-physical

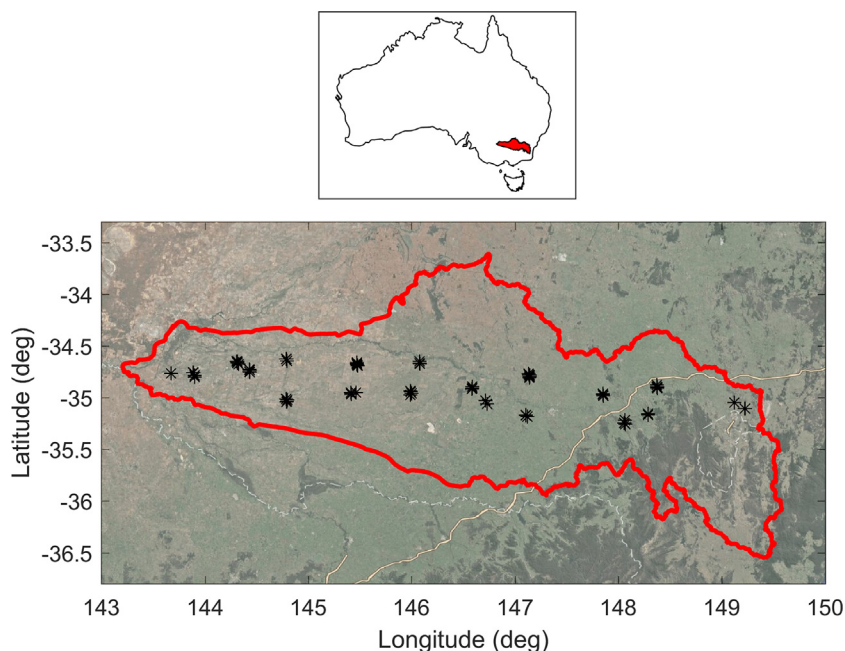


Fig. 1. Murrumbidgee River Catchment with marked locations of measured sites (asterisks).

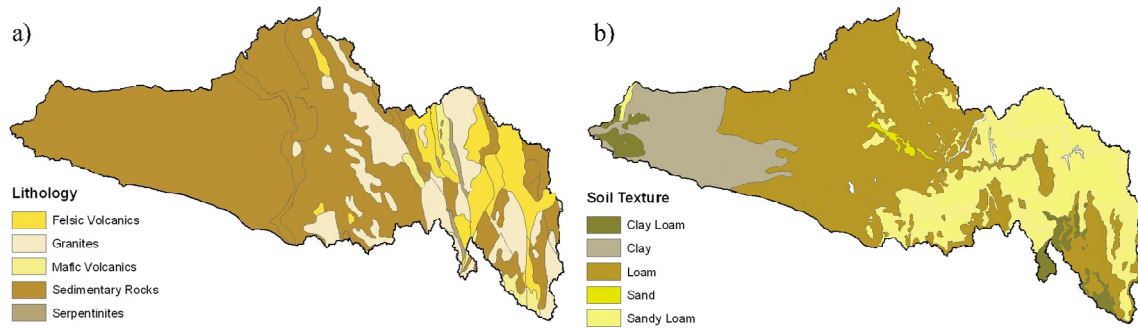


Fig. 2. Lithology (a) and soil texture (b) in the Murrumbidgee River Catchment (reproduced from Fig. 2 in [26]).

model of thermal conductivity  $\lambda$  ( $\text{W m}^{-1} \text{K}^{-1}$ ) [18]. The thermal conductivity of the soil ( $\lambda$ , in  $\text{W m}^{-1} \text{K}^{-1}$ ) was calculated according to [18]:

$$\lambda = \frac{4\pi}{u \sum_{j=1}^L \frac{P(x_{1j}, \dots, x_{kj})}{x_{1j} \lambda_{1(T)} r_1 + \dots + x_{kj} \lambda_{k(T)} r_k}} \quad (1)$$

where  $u$  is the number of parallel connections of soil particles treated as thermal resistors,  $L$  is the number of all possible combinations of particle configuration,  $x_1, x_2, \dots, x_k$  are the numbers of individual particles of a soil with thermal conductivity  $\lambda_1, \lambda_2, \dots, \lambda_k$  and particle radii  $r_1, r_2, \dots, r_k$  respectively and  $\sum_{i=1}^k x_{ij} = u$ ,  $j=1, 2, \dots, L$ ,  $P(x_{ij})$  is the probability of occurrence of a given soil particle configuration calculated from the polynomial distribution [29]:

$$P(x_{1j}, \dots, x_{kj}) = \frac{u!}{x_{1j}! \dots x_{kj}!} f_1^{x_{1j}} \dots f_k^{x_{kj}} \quad (2)$$

The condition  $\sum_{j=1}^L P(X = x_j) = 1$  must be fulfilled. The selection probability of a given particle  $f_i$ ,  $i = s, l, g$ , (solid, liquid, gas, respectively) in a single sample is determined by the soil's general properties. The values of  $f_s$ ,  $f_l$ , and  $f_g$  are taken individually for composing fractions of minerals and organic matter as  $f_s = 1 - \varphi$ , for liquids as  $f_l = \theta_v$ , and for air or gases as  $f_g = \varphi - \theta_v$ , inside the unitary volume with assumed porosity  $\varphi$  ( $\text{m}^3 \text{m}^{-3}$ ) and water content  $\theta_v$  ( $\text{m}^3 \text{m}^{-3}$ ).

The number of parallel and serial connections of thermal resistors in the model depends strongly on the water content and bulk density of the soil. Increase in volume fraction of water and bulk density results in a greater number of water bridges between the solid particles and a greater number of contact points, and thus contact area between the solid particles, respectively. The model adjusts the number of parallel connections of thermal resistors from 3 to 13, along with changing the ratio of water content in the unit of soil volume to its porosity and changing the spheres' radii  $r_k$  with the change of the organic matter content [18,25]:

$$r_k = 0.036f_o + 0.044, \quad (3)$$

where  $f_o$  ( $\text{m}^3 \text{m}^{-3}$ ) is the content of organic matter in a unit of volume.

The volumetric heat capacity  $C_v$  (in  $\text{J m}^{-3} \text{K}^{-1}$ ) was calculated using the empirical formulae proposed by de Vries [7]:

$$C_v = (2.0x_s + 2.51x_o + 4.19x_w) \cdot 10^6, \quad (4)$$

where  $x_s$ ,  $x_o$  and  $x_w$  ( $\text{m}^3 \text{m}^{-3}$ ) are the volumetric contributions of mineral and organic components and water, respectively. The thermal diffusivity  $\alpha$  ( $\text{m}^2 \text{s}^{-1}$ ) is calculated from the ratio:

$$\alpha = \lambda / C_v. \quad (5)$$

The calculation of the thermal conductivity according to the statistical-physical model was performed using ThermalWin [30]. The input data needed for the calculations consists of the soil mineralogical composition, organic matter content, porosity, temperature, and water content. Moreover, the statistical-physical model requires reference data on the thermal conductivity of quartz ( $\lambda_q$ ), other minerals ( $\lambda_m$ ), organic matter ( $\lambda_o$ ), water ( $\lambda_l$ ) and air ( $\lambda_g$ ) (summarized in Table 1). In this approach, the transport of latent heat due to moisture movement was neglected.

Two different systems, Australian/ISSS and USDA/FAO [24] were taken into account here for the soil granulometry classification. The difference between them is in the sand and silt fraction classifications. According to the Australian/ISSS system, sands particles are of size 0.02–2 mm and silt 0.002–0.02 mm, while according to the USDA/FAO sand is 0.05–2 mm and silt 0.002–0.05 mm. For both systems clay is classified as particles smaller than 0.002 mm.

The contents of the main soil mineralogical components, mainly quartz and other minerals, can be obtained by direct measurements or by estimates based on soil granulometric fractions [7,18]. Quartz content was estimated by taking into account the sand and finer fraction of the examined soils. The granulometric fractions were defined according to the classifications used in Australia and with the USDA conventions. Measured soil thermal conductivities were compared to the computed values from the Usovicz's statistical-physical model. Indicators of agreement between measured and calculated values were analyzed. The contents of quartz, other minerals, water and air obtained from gravimetric measurements were used as input for the calculation of the thermal conductivity of the soil. For the estimation of quartz contents only those granulometric fractions for which the correspondence between measured and calculated thermal conductivities were the most satisfactory were selected. In detail, the coefficient of determination ( $R^2$ ) was the biggest, the slope of the linear

Table 1

Expressions and values for components used in calculating the thermal conductivity of soils ( $T$  in  $^\circ\text{C}$ ).

Source	Component	Thermal conductivity	Expression/values ( $\text{W m}^{-1} \text{K}^{-1}$ )
De Vries [7]	quartz	$\lambda_q$	$9.103 - 0.028 T$
	other minerals	$\lambda_{mi}$	2.93
De Vries [7]	organic matter	$\lambda_o$	0.251
Kimball et al. [31]	water	$\lambda_w$	$0.552 + 2.34 \cdot 10^{-3} T - 1.1 \cdot 10^{-5} T^2$
Kimball et al. [31]	air	$\lambda_g$	$0.0237 + 0.000064 T$

regression describing the dependence of the calculated and the measured conductivity was close to 1, its intercept was near zero, and the mean square error was low. The remaining granulometric fractions were treated as “other minerals”.

2.2. Spatial variability of soil physical properties

The analyses of the soil property’s spatial distribution is based on geostatistical methods. However, as the basic requirement of a geostatistical analysis is to use data that is characterized by a normal (Gaussian) distribution, the mean, variance, skewness, and kurtosis were computed to determine skewness in the distribution, and to characterize the soils. The foremost property of a Gaussian distribution is its symmetry, quantified by skewness equal or close to zero. In the case of a significant asymmetry (i.e. positive or negative skew) in the analyzed datasets, a root square (sqrt.) or logarithmic (ln) transformation was performed, depending on which one brought the datasets closer to a Gaussian distribution. For every examined soil property, empirical semivariograms  $\gamma(h)$  were determined and the theoretical models adjusted to match the empirical semivariograms. The empirical semivariograms  $\gamma(h)$  for distance  $h$  were calculated from:

$$\gamma(h) = \frac{1}{2N(h)} \sum_{i=1}^{N(h)} [z(x_i) - z(x_i + h)]^2, \tag{6}$$

where  $N(h)$  is the number of pairs of points  $z(x_i)$  separated by the distance  $h$ . The empirical semivariograms provide information on the spatial autocorrelation of datasets. However, it does not provide information for all possible distances as the values are discrete. For this reason it was necessary to fit a model [32,33]. The best fit to the data examined in this paper was reached when the spherical isotropic model was used. It is a modified polynomial function for which the semivariogram reaches an asymptote at a particular distance  $A_0$  (called “range”). The formula of this model is:

$$\gamma(h) = \begin{cases} C_0 + C \cdot \left[ 1.5 \frac{|h|}{A_0} - 0.5 \left( \frac{|h|}{A_0} \right)^3 \right] & |h| \leq A_0 \\ C_0 + C & h > A_0 \end{cases}, \tag{7}$$

where  $\gamma(h)$  is the semivariance for the internal distance class  $h$ , with  $h$  being the lag interval,  $C_0$  the nugget variance  $\geq 0$ ,  $C$  the structural variance  $\geq C_0$ ,  $A_0$  the range parameter, and  $C_0 + C$  the sill. In the case of the spherical model the effective range  $A = A_0$ .

Estimations of the soil properties in places where no samples have been taken were conducted applying the ordinary kriging method [32,33], resulting in spatial distributions, i.e. maps of bulk density, water content, and soil thermal properties. The use of the

geostatistical method for the analysis of soil thermal properties across entire catchment seems to be controversial due to extended area and rain events occurrence during the campaign, however it was utilized as an attempt to estimate roughly spatial dependence of the examined properties.

3. Results and discussion

The granulometric fractions contents are shown in Fig. 3a, for which estimates of quartz and other minerals were made in Fig. 3b according to method described in the literature [7,18,25].

According to the Australian granulometry classification, the average particle size distribution of the samples collected across the Murrumbidgee River catchment was 65.6% sand, 21.2% silt, and 13.2% clay. According to the USDA classification, sand content was on average 13.2% smaller than that according to the Australian classification, and volumetric quartz content was 12.9% smaller (Fig. 3b). According to the Australian classification quartz content was estimated to be 64.3%, while according to USDA it was 51.4%. Other mineral contents in the soil were assumed to complement to 100%. Similarities in sand and quartz contents for coarse-grain Australian soils were also observed by other authors [5].

Fig. 4 shows the comparison of the thermal conductivity calculated and measured with estimated contents of quartz and other

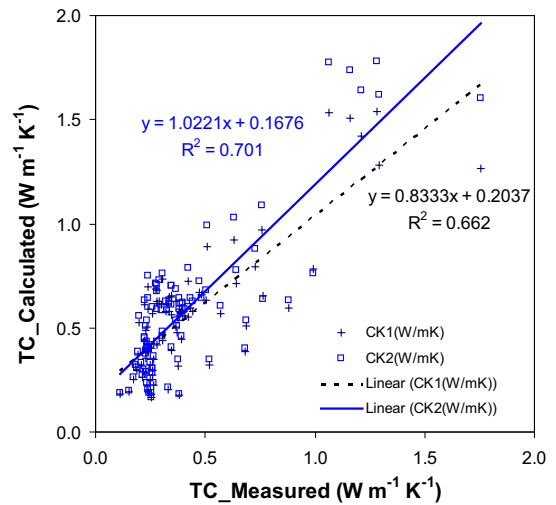


Fig. 4. Thermal conductivity of soil (TC) calculated vs. measured. Calculations are according to USDA (CK1, black) and Australian (CK2, blue) classification of granulometric fractions.

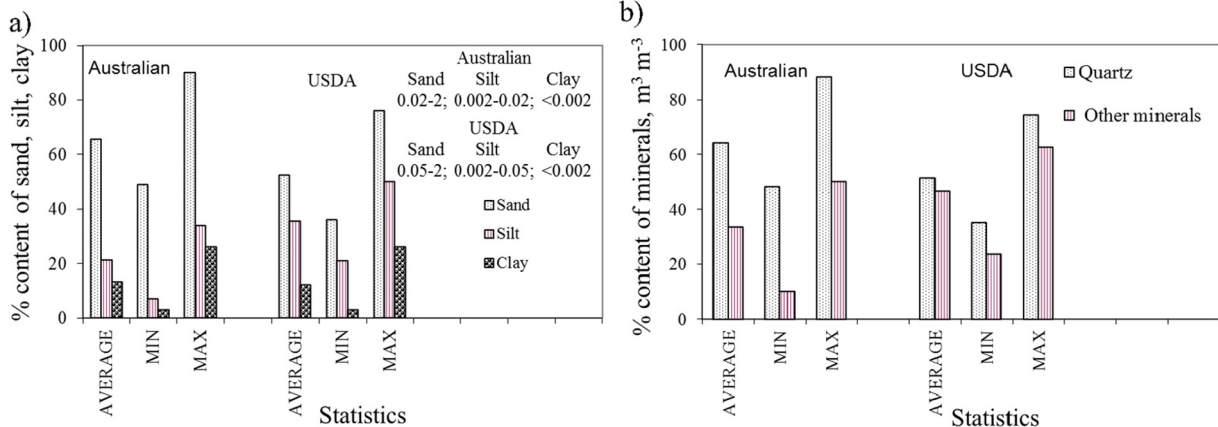


Fig. 3. Granulometric fractions content (a) and volumetric content of quartz and other minerals (b) according to Australian and USDA granulometry classification.

minerals from both the Australian and USDA particle size distribution classifications. The coefficient of determination of the thermal conductivity calculated for the estimated quartz composition against measured values was slightly (0.04) larger for the Australian particle size distribution classification than for the USDA classification. Similarly, better performance was obtained for the regression equations for the Australian classification than for the USDA. Mean square errors ( $\sigma_b$ ) were similar, although slightly higher for the Australian classification (0.256) than USDA (0.219). For further examinations the Australian classification was chosen due to the higher  $R^2$  and the linear regression slope being closer to 1 when compared to the USDA classification. Apparently, higher quartz content estimated via Australian classification brought Usovicz's statistical-physical model closer to the measured values than the one predicted using USDA.

Quartz and other minerals contents, organic matter content (about 2%), soil water content measured by the gravimetric method and the Hydra Probe sensor, soil bulk density and the density of the soil solid phase were all used to estimate the spatial distribution of thermal properties of the soils in the Murrumbidgee River catchment. A comparison of the HDAS (Hydra Probe) [26] data acquisition system and gravimetric soil water content measurement methods was made (Fig. 5). The coefficient of determination ( $R^2$ ) was almost 0.9, indicating good agreement between both methods. However, linear regression slope equal to 0.92 and positive intercept indicates that the values determined by the gravimetric method were slightly higher than those measured by the Hydra Probe sensor. Dispersion of the values, expressed by the root mean square error, was about 0.032 ( $\text{m}^3 \text{m}^{-3}$ ). Large relative discrepancies appeared when soil water content was low, which may be caused by problems related to the contact between soil and probe under dry conditions. This phenomenon was also observed by other studies [34].

Soil bulk density was between 0.94 and 1.61  $\text{Mg m}^{-3}$  with the standard deviation approximately 0.16  $\text{Mg m}^{-3}$ . The variation, depicted by coefficient of variation, was the smallest from all examined variables (approx. 13%). Mean value and median were similar. Soil bulk density distribution was slightly asymmetrical, skewed to lower values.

Soil water content (from both methods) was characterized by the highest variability of about 80% and a strong positive skewness of the distribution, which was mainly due to two significant rain events that occurred during the field campaign [26]. Very small water content (well below 0.1  $\text{m}^3 \text{m}^{-3}$ ) was observed in the arid

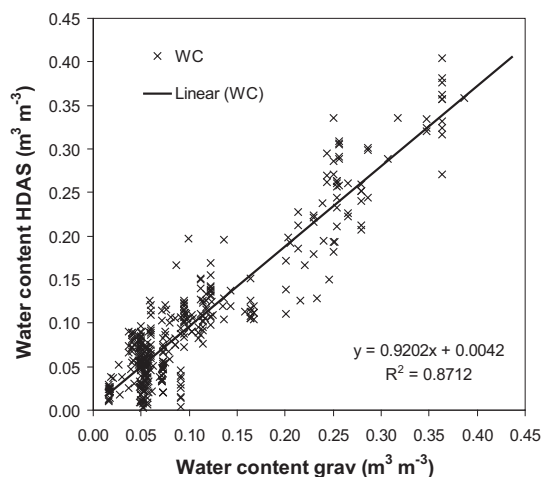


Fig. 5. Water content (WC) measured by Hydra Probe (HDAS) vs. gravimetric water content (grav).

western part of the catchment at the start of the campaign, which took place at the end of the so-called Millennium Drought [36]. Soil water content above 0.3  $\text{m}^3 \text{m}^{-3}$  was observed in the more humid eastern part of the catchment following a significant rain event during the middle of the campaign (up to 60 mm in a day [26]). Positive skewness, mentioned before, was occurring because high moisture contents were observed, but much less frequent than dry soil states. The soil water content distribution was far from Gaussian (normal) distribution, as indicated by the non-zero skewness and a big difference between the mean value and median. In order to meet the assumptions necessary for geostatistical analysis, the soil water content data was transformed using the natural logarithm transformation. As a result, the asymmetry decreased and mean value became closer to the median, thus making the soil water content distribution resemble a normal (Gaussian) distribution.

Among the examined soil thermal properties, thermal conductivity had the largest variability (CV approximately 77%), while heat capacity had the smallest variability (CV approximately 29%). The variability of thermal diffusivity was approximately 50%. Distributions of thermal conductivity and heat capacity, as well as soil water content, were strongly skewed towards higher values. Evident impact of the soil water content on thermal properties of the soil was observed. The values of thermal conductivity and heat capacity rose with growing water content. Thermal conductivity was between 0.06 and 2.4  $\text{W m}^{-1} \text{K}^{-1}$ , while heat capacity was from 0.78 to 2.7  $\text{MJ m}^{-3} \text{K}^{-1}$ . The increase in the bulk density of the soil also resulted in increased values of thermal properties of the soil, but it had a greater effect on the thermal conductivity than on the thermal capacity. This was due to the impact of the bulk density on these properties. The increase in the soil bulk density resulted in an increase in the intercept of the linear relationship between soil water content and heat capacity in the direction of higher values of heat capacity [37]. In the case of thermal conductivity, the increase in bulk density caused an increase in thermal conductivity and significantly changed the nonlinear dependence between thermal conductivity and soil water content.

The statistical distributions of thermal diffusivity were slightly skewed to the right, in contrast to the left-skewed distributions of conductivity and heat capacity. The impact on thermal diffusivity distribution may come from soil moisture and bulk density, and also from the internal nature of thermal diffusivity, which reaches distinctive saturation points for different moisture and soil density conditions. In the case of thermal diffusivity, it was found that the distributions were similar to the normal distribution. The thermal conductivity and heat capacity, which deviate from the normal distribution, were transformed: the first feature by the square root transform, natural logarithm transform of the second. Transformed data had reduced asymmetry and was closer to a normal distribution than the raw data, thus allowing geostatistical analyses to be conducted, i.e. to obtain semivariograms and estimate the spatial distribution of the studied variables using the kriging method. Bulk density and thermal diffusivity of the soil did not require transformations because the distributions were similar to the normal (Gaussian) distribution.

### 3.1. Geostatistical analyses

For each of the examined soil properties, experimental semivariograms were calculated and models fitted to determine the nugget, sill, and range (Table 3). In a reasonable approximation, the nature of changes of all the studied soil properties in the Murrumbidgee River catchment could be described by a spherical model of semivariance. Geostatistical analyses revealed that soil bulk density had the smallest range (sill = 0.026) while soil water content had the biggest (sill = 0.621).

**Table 2**  
Statistical summary of bulk density, soil water content and thermal properties in the Murrumbidgee River Catchment.

Properties <sup>a</sup>	N	Mean	Median	Minimum	Maximum	Standard Deviation	CV (%)	Skewness	Kurtosis
BD (Mg m <sup>-3</sup> )	367	1.278	1.286	0.944	1.613	0.163	12.8	-0.212	-0.676
WCgrav (m <sup>3</sup> m <sup>-3</sup> )	367	0.109	0.073	0.016	0.386	0.087	79.6	1.464	1.204
WCHDAS (m <sup>3</sup> m <sup>-3</sup> )	367	0.105	0.081	0.002	0.404	0.086	81.9	1.422	1.409
TCgrav (W m <sup>-1</sup> K <sup>-1</sup> )	367	0.805	0.749	0.123	2.410	0.599	74.4	0.929	0.003
TCHDAS (W m <sup>-1</sup> K <sup>-1</sup> )	367	0.803	0.758	0.061	2.390	0.616	76.7	0.761	-0.282
HCgrav (MJ m <sup>-3</sup> K <sup>-1</sup> )	367	1.459	1.380	0.929	2.650	0.411	28.2	1.064	0.488
HCHDAS (MJ m <sup>-3</sup> K <sup>-1</sup> )	367	1.441	1.417	0.779	2.740	0.424	29.4	0.873	0.390
TDgrav (m <sup>2</sup> s <sup>-1</sup> )	367	4.90E-07	4.55E-07	1.33E-07	1.10E-06	2.50E-07	51.1	0.239	-1.041
TDHDAS (m <sup>2</sup> s <sup>-1</sup> )	367	4.87E-07	5.26E-07	7.74E-08	1.15E-06	2.72E-07	55.8	0.109	-1.220

<sup>a</sup> BD – bulk density, grav – gravimetric method, HDAS – Hydra Probe data acquisition system sensor, WCgrav – water content determined by gravimetric method, WCHDAS – water content measured by Hydra Probe meter, TCgrav – thermal conductivity calculated with gravimetric data, TCHDAS – thermal conductivity calculated with Hydra Probe data, HCgrav – Heat capacity calculated with gravimetric data, HCHDAS – Heat capacity calculated with Hydra Probe data, TDgrav – thermal diffusivity calculated with gravimetric data, TDHDAS – thermal diffusivity calculated with Hydra Probe data.

**Table 3**  
Geostatistical properties of the investigated parameters.

	Bulk density	Water content		Thermal conductivity		Heat capacity		Thermal diffusivity	
		grav	HDAS	grav	HDAS	grav	HDAS	grav	HDAS
Variogram model type	spherical	spherical	spherical	spherical	spherical	spherical	spherical	spherical	spherical
Nugget (C <sub>0</sub> )	0.014	0.121	0.138	0.020	0.033	0.012	0.020	0.014	0.017
Sill (C <sub>0</sub> + C)	0.026	0.621	0.619	0.114	0.122	0.070	0.069	0.076	0.086
Range (A)	1.362	2.223	2.160	2.446	2.299	2.153	2.431	2.292	2.187

**Table 4**  
Cross-validation analysis – kriging effective parameters.

Soil properties <sup>a</sup>	Regression slope	Intercept	Standard error	R <sup>2</sup>
BD (Mg m <sup>-3</sup> )	0.958	0.054	0.176	0.274
WCgrav (m <sup>3</sup> m <sup>-3</sup> )	1.002	0.004	0.066	0.746
WCHDAS (m <sup>3</sup> m <sup>-3</sup> )	1.013	0	0.078	0.682
TCgrav (W m <sup>-2</sup> K <sup>-1</sup> )	1.015	0	0.054	0.817
TCHDAS (W m <sup>-1</sup> K <sup>-1</sup> )	1.031	0	0.07	0.737
HCgrav (J m <sup>-3</sup> K <sup>-1</sup> )	0.999	-0.003	0.056	0.804
HCHDAS (J m <sup>-3</sup> K <sup>-1</sup> )	1.029	-0.048	0.072	0.723
TDgrav (m <sup>2</sup> s <sup>-1</sup> )	0.996	0.001	0.063	0.761
TDHDAS (m <sup>2</sup> s <sup>-1</sup> )	0.995	0.002	0.073	0.704

<sup>a</sup> BD – bulk density, grav – gravimetric method, HDAS – Hydra Probe data acquisition system sensor, WCgrav – water content determined by gravimetric method, WCHDAS – water content measured by Hydra Probe meter, TCgrav – thermal conductivity calculated with gravimetric data, TCHDAS – thermal conductivity calculated with Hydra Probe data, HCgrav – Heat capacity calculated with gravimetric data, HCHDAS – Heat capacity calculated with Hydra Probe data, TDgrav – thermal diffusivity calculated with gravimetric data, TDHDAS – thermal diffusivity calculated with Hydra Probe data.

Thermal properties computed for the two distributions of soil water content (obtained from gravimetric method and Hydra Probe moisture meter) were analyzed separately in order to examine how the chosen method of soil water content determination influences the distribution of heat capacity, thermal diffusivity and conductivity. Dispersion (sill) values for the heat capacity, thermal diffusivity and thermal conductivity were at a similar level, with maximum values of 0.070, 0.086, 0.122 respectively. Nuggets of soil water content and thermal properties calculated from the Hydra Probe soil water content data were bigger than those obtained from soil water content data obtained via the gravimetric method. It indicates that soil properties derived from the Hydra Probe sensor are less sensitive to soil water content changes, compared to the gravimetric method, which is often taken as the reference method. Geostatistical analyses also enable calculation of the so-called range (A), indicating the distance over which there is a spatial dependence of the examined feature. In this paper range is expressed in degrees (°) with a reference to the point coordinates taken (lat/lon, WGS 84). One degree (1°) on that latitude is about 100 km. Soil bulk density had the smallest range of spatial dependence (A = 1.362°). Other properties were characterized by

significantly higher ranges (A from 2.153° to 2.446°) (Table 3). Spatial variability of all the examined parameters was described by a spherical semivariogram model.

Semivariogram models obtained from the data analysis were used in the kriging method to estimate the values of individual properties in the areas where these features were not measured. To check the reliability of kriging estimations, cross-validation was conducted at points where the measurements were made. Results of the cross-validation are shown in Table 4. Almost all of the examined variables were estimated with satisfactory accuracy. Most of the regression slopes were close to 1 and intercepts close to zero. Standard errors and coefficients of determination (R<sup>2</sup>) were satisfactory, all with the exception of bulk density. Accuracy parameters of models obtained from properties calculated from gravimetric method of water content determination were slightly better than those from Hydra Probe measurements. The parameters obtained from the cross-validation analysis indicate that the maps (Figs. 6–10) estimated from the water content gravimetric data are more accurate and diverse than maps obtained from Hydra Probe measurements. The latter are “smoother”, however, have a similar basic pattern as the first.

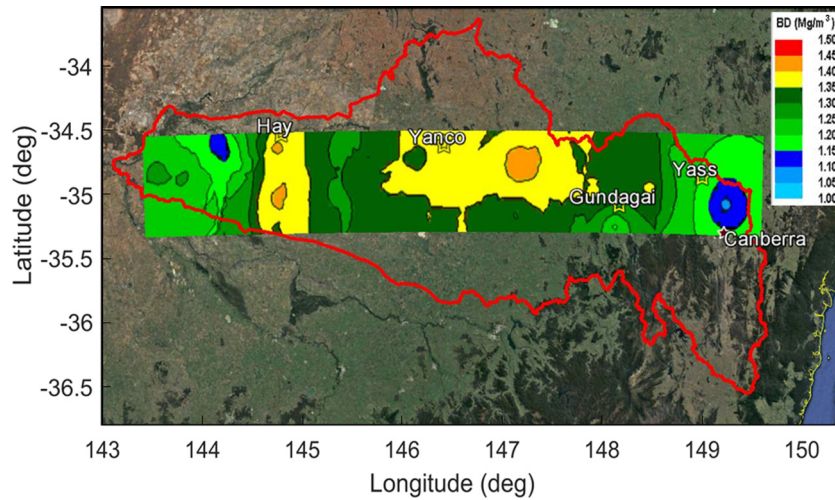


Fig. 6. Spatial distribution of soil bulk density in the Murrumbidgee River catchment, Australia. Background from Google Earth [38].

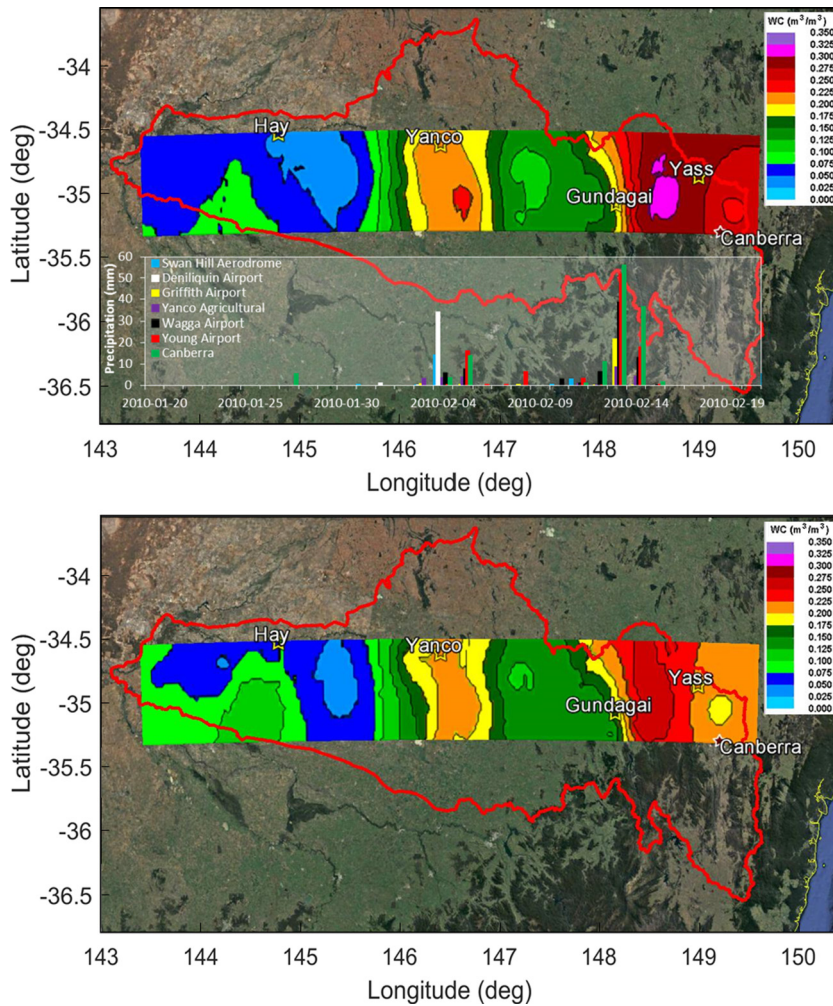
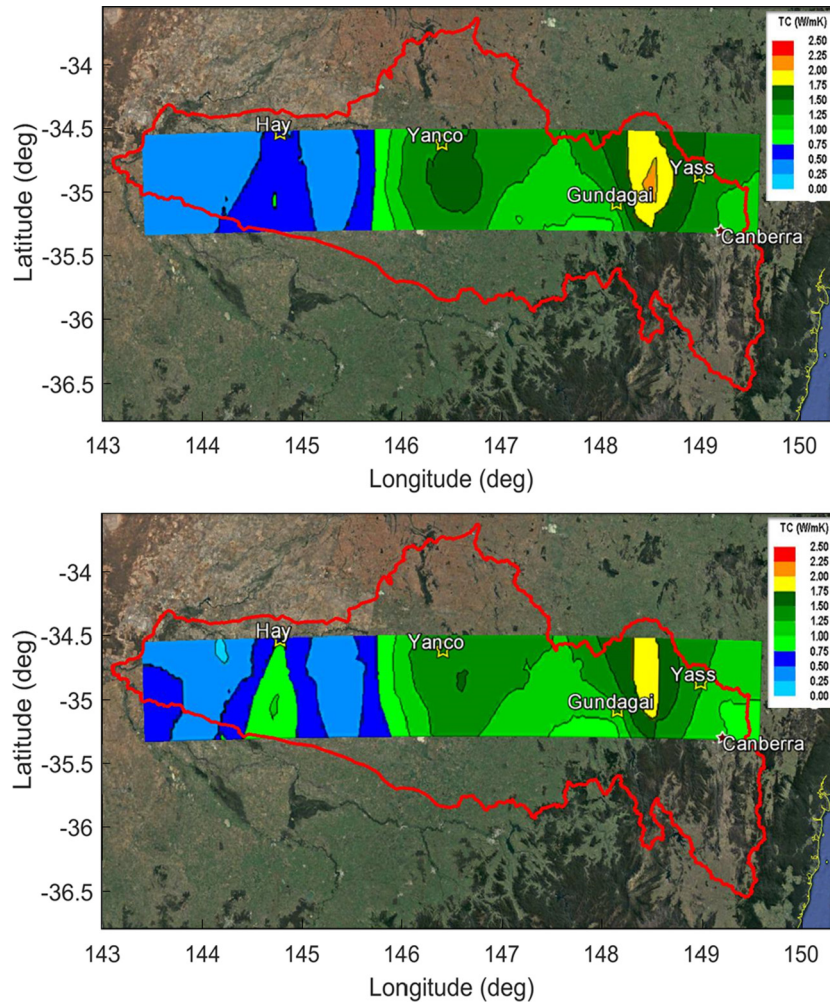


Fig. 7. Spatial distribution of water content in the Murrumbidgee River Catchment, Australia obtained from gravimetric method (upper panel) and measured with Hydra Probe II (lower panel). Superimposed graph of precipitation (data obtained from local meteorological stations [35]) is adjusted in a way to indicate the date and location of the most significant rainfalls. Background from Google Earth [38].

### 3.2. Derived soil property maps

Figs. 6–10 present 2 D maps (obtained from ordinary kriging method) of bulk density, water content, thermal conductivity, heat

capacity and thermal diffusivity in the Murrumbidgee River catchment. The spatial distributions of the thermal properties (Figs. 8–10) were associated with water content in the soil and its bulk density (Figs. 6 and 7).



**Fig. 8.** Spatial distribution of soil thermal conductivity (TC) in the Murrumbidgee River Catchment, Australia. TC modelled using water content obtained from gravimetric method (upper panel) and measured with Hydra Probe II (lower panel). Background from Google Earth [38].

### 3.3. Soil bulk density

The bulk density of the soil, estimated by the kriging method (Fig. 6), has a range from 1.1 to 1.4 Mg m<sup>-3</sup>. The highest bulk densities were observed in the central part of the Murrumbidgee River catchment, varying slightly between 1.3 and 1.4 Mg m<sup>-3</sup>. Lower bulk density values (from 1.1 to 1.2 Mg m<sup>-3</sup>) were observed in the eastern and western parts of this area. The ranges of estimated values are lower than the measured values in Table 2, because extreme values of soil bulk density were rare, thus they have been taken into account to a lesser extent during the kriging estimation than those that occurred more frequently. The spatial pattern of the bulk density distribution for the Murrumbidgee River catchment soils is clearly reflected in the spatial distribution of thermal diffusivity, and a bit less in the thermal conductivity distribution pattern.

### 3.4. Soil water content

Spatial distributions of the soil water content obtained from the gravimetric method (Fig. 7 upper panel) and measured by the Hydra Probe (Fig. 7 lower panel) were examined. The soil water content reflected the current moisture conditions during the one month measurements acquisition where the extreme dry conditions were followed by intense rainfall during the AACES

campaign. During the campaign, the measurements were conducted from West to East. There was low soil water content values in the western part of the study area with an increase in the value towards the East, mostly due to the heavy rainfall in the middle of the campaign (from the central region on eastwards). In the western part of the examined area, soil water content obtained from the gravimetric method (mean approx. 0.05 m<sup>3</sup> m<sup>-3</sup>) was lower than that obtained by the Hydra Probe (approx. 0.1 m<sup>3</sup> m<sup>-3</sup>). In the central and eastern part, the situation was reversed: gravimetric method indicated ~0.325 m<sup>3</sup> m<sup>-3</sup> while Hydra Probe ~ 0.30 m<sup>3</sup> m<sup>-3</sup>. This was due to the different accuracies of both methods: Comparing to gravimetric (which is reference) method, Hydra Probe overestimated soil water content when the soil was dry and underestimated it when the soil was wet, as shown by the linear regression equation in Fig. 5. The pattern of the soil water content distribution in the Murrumbidgee River catchment is reflected by the spatial distributions of the heat capacity, thermal conductivity and the thermal diffusivity.

### 3.5. Soil thermal conductivity

Soil thermal conductivity distribution in the Murrumbidgee River Catchment mainly reflects the distribution of soil water content from both examined methods (Fig. 7). In the western part of the studied area the lowest values of conductivity (~0.25 W m<sup>-1</sup>

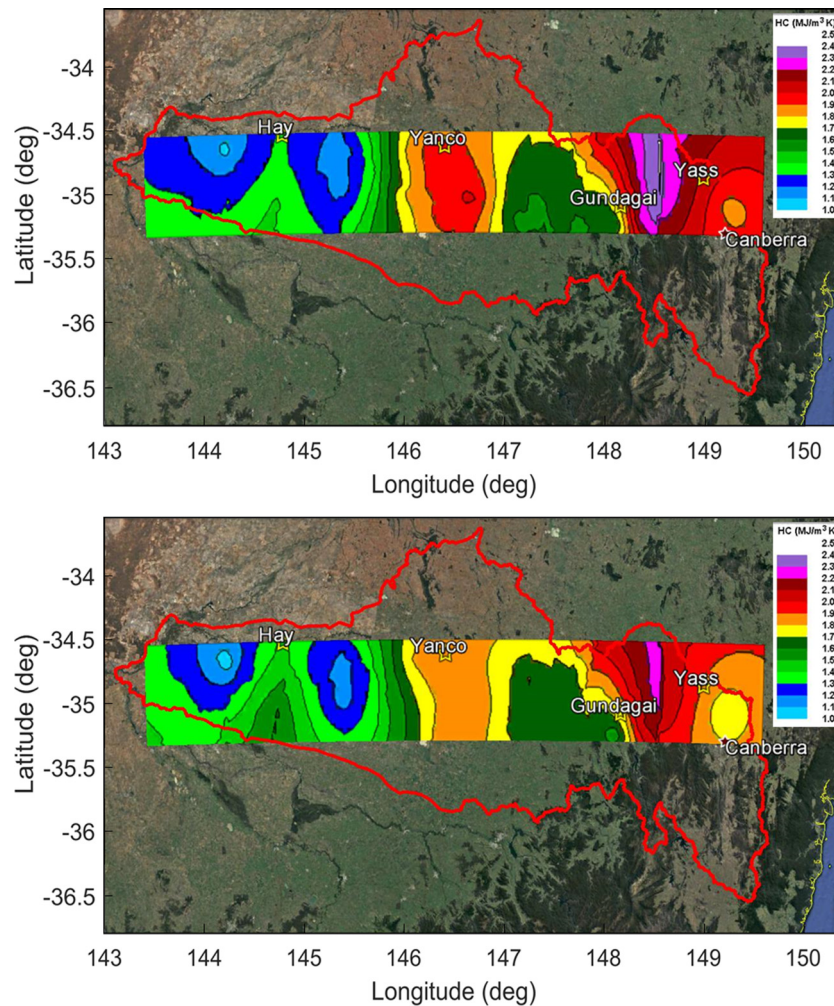


**Fig. 9.** Spatial distribution of soil heat capacity (HC) in the Murrumbidgee River Catchment, Australia. HC modelled using water content obtained from gravimetric method (upper panel) and measured with Hydra Probe II (lower panel). Background from Google Earth [38].

$\text{K}^{-1}$ ) were recorded, increasing towards the East ( $\sim 2.25 \text{ W m}^{-1} \text{ K}^{-1}$ ). In the western part, smaller values of conductivity were observed when it had been calculated from the soil water content data received from the gravimetric method than when obtained from the Hydra Probe. The reverse situation occurred in the East. In the central part of the catchment, where soil water content after saturation began to fall and then rise again towards the East, a positive impact of the bulk density can be noticed on the soil thermal conductivity. In this area, the decline of the conductivity was not as intense as decline of soil water content because the bulk density of the soil in this area was significant and it led to a significant increase in the conductivity, which was observed also by other authors [5,34].

### 3.6. Soil heat capacity

Spatial diversity of heat capacity in the Murrumbidgee River catchment (Fig. 9) was more related to the soil water content than to the soil bulk density. Here, as in the case of thermal conductivity, in the western part of the test area the lowest values of heat capacity were reported ( $\sim 1.1 \text{ MJ m}^{-3} \text{ K}^{-1}$ ) and increased towards the east ( $\sim 2.4 \text{ MJ m}^{-3} \text{ K}^{-1}$ ). The minimum value is the same as found by other authors for dry sandy-loam soils [34]. In the western part, smaller values of heat capacity were observed when it was calculated from the water content data received from the

gravimetric method than soil thermal capacities calculated from data from the Hydra Probe soil water content. Again, the reverse situation occurred in the East. The spatial distribution of the heat capacity was not clearly reflected in the spatial distribution of the bulk density, but it was reflected in soil water content distribution.

### 3.7. Thermal diffusivity

The spatial distribution of thermal diffusivity in the Murrumbidgee River catchment (Fig. 10) is very similar to the distribution of soil bulk density. Soil water content had rather low impact on the value of soil thermal diffusivity and was only partially reflected in its spatial distribution. In the western part of the study area the lowest values of thermal diffusivity were recorded ( $\sim 0.3 \times 10^{-6} \text{ m}^2 \text{ s}^{-1}$ ) and they were growing towards the East ( $\sim 1.0 \times 10^{-6} \text{ m}^2 \text{ s}^{-1}$ ). In the middle part of the studied area, where soil bulk density was the highest and soil water content reached its maximum and then decreased, thermal diffusivity reached its highest values. A slight decrease in diffusivity in the central part of the catchment can be observed where the soil water content decreases. It can be concluded that the bulk density of the soil had dominant influence on thermal diffusivity. However, when the soil water content was high it has also an impact on the value of thermal diffusivity.

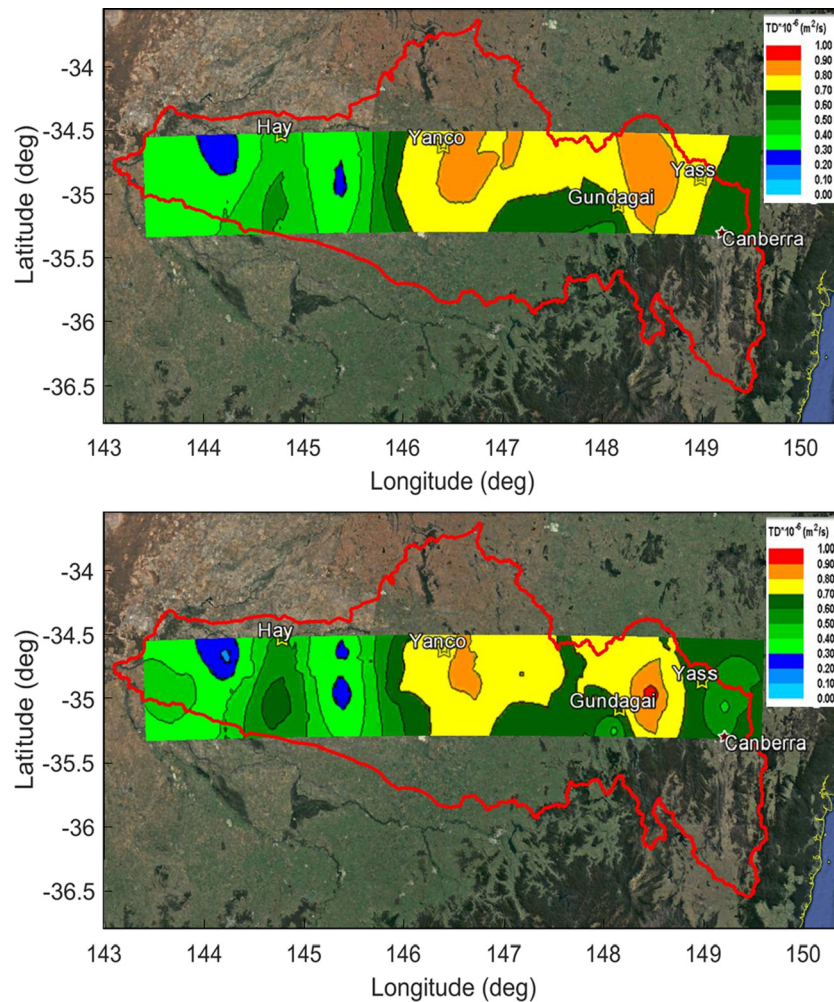


**Fig. 10.** Spatial distribution of soil thermal diffusivity (TD) across the Murrumbidgee River Catchment, Australia. TD modelled using water content obtained from gravimetric method (upper panel) and measured with Hydra Probe II (lower panel). Background from Google Earth [38].

The nature of the variation of thermal diffusivity, which is highly non-linear, is associated with conductivity and heat capacity dynamics that change with soil water content and density. Heat capacity increases linearly with increasing soil water content and goes towards higher values of capacitance with an increase in bulk density, but does not change its nature and remains linear. However, the thermal conductivity has a large non-linearity with the change of soil water content and bulk density. Depending on the range of the thermal conductivity changes, with a constant change in heat capacity, a thermal conductivity value “saturation” can be observed, which is characteristic for the thermal diffusivity at the specified soil water content and bulk density. For the specific bulk density and soil water content, saturation of the thermal diffusivity value is observed. Increasing soil bulk density while changing soil water content causes the thermal diffusivity values saturation shift towards the lower soil water content values. Comparison with the spatial distributions of bulk density and soil water content indicates that the spatial distribution of the thermal diffusivity in the middle of the area was around its saturation.

#### 4. Conclusions

The soil bulk density, water content and soil thermal properties in the Murrumbidgee River catchment, Australia, in the middle of the Australian summer (from 18 January to 21 February 2010)

were presented. The quartz and other minerals contents in the Murrumbidgee River catchment have been assessed according to the Australian and USDA particle size distribution classifications, via modelling of heat conductivity by the Usovicz’s statistical-physical model and comparing them with the conductivity values measured during the campaign. It was shown that it can be estimated more accurately from the Australian soil granulometry than USDA classification.

For the defined quartz and other minerals contents, the soil thermal properties were mainly governed by water content and bulk density of soil. The variability was the lowest for the bulk density (CV = 13%) and successively increased for the heat capacity (29%), thermal diffusivity (56%), thermal conductivity (77%) and water content (82%).

By using geostatistical analyses it was possible to identify areas of different thermal properties of the soil in the Murrumbidgee River Catchment. Knowledge of the spatial distribution of thermal properties may be useful to determine the spatial distribution of the heat flux density, which is one of the components of the heat balance. Quartz and water content and the bulk density of soil were the main factors that affected the thermal properties of soil. Greater diversity of thermal properties was observed for the data obtained from the gravimetric method than the measured by Hydra Probe, resulting in flatter distributions for the latter. The spatial distributions of conductivity and heat capacity were governed by the soil water content pattern, while the thermal

diffusivity was mainly driven by the bulk density distribution. Knowledge of the spatial distribution of soil bulk density and water content can be useful to develop precise agronomic practices to improve the thermal properties of the soil and the quality and efficiency of cultivated plants in the considered area.

In the future, knowing the physical properties of the soil (from existing databases or new measurements) and soil water content it will be possible to estimate the thermal properties of soil, possibly even on large scales when using data obtained from satellites or widespread ground-based campaigns.

## Acknowledgements

The work was partially financed through ESA (European Space Agency) Contracts under the PECS (Plan for European Cooperating States): i) “SWEX-R, Soil Water and Energy Exchange/Research” (No.98084) and ii) “ELBARA\_PD (Penetration Depth)” (No. 4000107897/13/NL/KML) and iii) Australian Research Council funding from DP0879212.

## Conflict of interest

The authors declare that there is no conflict of interest.

## References

- [1] D.M. Murphy, S. Solomon, R.W. Portmann, K.H. Rosenlof, P.M. Forster, T. Wong, An observationally based energy balance for the Earth since 1950, *J. Geophys. Res.* 114 (D17) (2009) 107, <http://dx.doi.org/10.1029/2009JD012105>.
- [2] A. Verhoef, *Agric. For. Meteorol.* 123 (2004) 221–236, <http://dx.doi.org/10.1016/j.agrformet.2003.11.005>.
- [3] M. Lehnert, M. Vysoudil, P. Kladio, Semi-stationary measurement as a tool to refine understanding of the soil temperature spatial variability, *Int. Agrophys.* 29 (4) (2015) 449–457, <http://dx.doi.org/10.1515/intag-2015-0038>, ISSN (Online) 2300-8725.
- [4] J. Bachmann, R. Horton, T. Ren, R.R. Van der Ploeg, Comparison of the thermal properties of four wettable and four water-repellent soils, *Soil Sci. Soc. Am. J.* 65 (2001) 1675–1679.
- [5] D. Barry-Macaulay, A. Bouazza, R.M. Singh, B. Wang, P.G. Ranjith, Thermal conductivity of soils and rocks from the Melbourne (Australia) region, *Eng. Geol.* 164 (2013) 131–138.
- [6] C. Yang, M. Sakai, S.B. Jones, Inverse method for simultaneous determination of soil water flux density and thermal properties with a penta-needle heat pulse probe, *Water Resour. Res.* 49 (2013) 5851–5864, <http://dx.doi.org/10.1002/wrcr.20459>.
- [7] D.A. de Vries, Thermal properties of soils, in: W.R. van Wijk (Ed.), *Physics of plant environment*, North-Holland, Amsterdam, 1963, pp. 210–235.
- [8] F. Gori, S. Corasaniti, Experimental measurements and theoretical prediction of the thermal conductivity of two- and three-phase water/olivine systems, *Int. J. Thermophys.* 24 (5) (2003) 1339–1353.
- [9] S. Nikoosokhan, H. Nowamooz, C. Chazallon, Effect of dry density, soil texture and time-spatial variable water content on the soil thermal conductivity, *Geomech. Geoen.* (2016), <http://dx.doi.org/10.1080/17486025.2015.1048313>.
- [10] T.E. Ochsner, R. Horton, T. Ren, A New Perspective on Soil Thermal Properties Journal Paper No. J-19021 of the Iowa Agriculture and Home Economics Experiment Station, Ames, IA, Project No. 3287. Supported by the Hatch Act and the State of Iowa, *Soil Sci. Soc. Am. J.* 65 (2001) 1641–1647, <http://dx.doi.org/10.2136/sssaj2001.1641>.
- [11] B. Usovicz, J. Lipiec, W. Marczewski, A. Ferrero, Thermal conductivity modelling of terrestrial soil media – a comparative study, *Planet. Space Sci.* 54 (11) (2006) 1086–1095, <http://dx.doi.org/10.1016/j.pss.2006.05.018>.
- [12] L.J.S. Halloran, G.C. Rau, M.S. Andersen, Heat as a tracer to quantify processes and properties in the vadose zone: a review, *Earth-Sci. Rev.* 159 (2016) 358–373, <http://dx.doi.org/10.1016/j.earscirev.2016.06.009>.
- [13] O. Nusier, N. Abu-Hamdeh, Laboratory techniques to evaluate thermal conductivity for some soils, *Heat Mass Transf.* 39 (2) (2003) 119–123.
- [14] T.E. Ochsner, R. Horton, T. Ren, Simultaneous water content, air-filled porosity, and bulk density measurements with thermo-time domain reflectometry, *Soil Sci. Soc. Am. J.* 65 (2001) 1618–1622.
- [15] T.E. Ochsner, R. Horton, T. Ren, A new perspective on soil thermal properties, *Soil Sci. Soc. Am. J.* 65 (2001) 1641–1647.
- [16] T. Ren, K. Noborio, R. Horton, Measuring soil water content, electrical conductivity and thermal properties with a thermo-time domain reflectometry probe, *Soil Sci. Soc. Am. J.* 63 (1999) 450–457.
- [17] V.R. Tarnawski, W.H. Leong, Thermal conductivity of soils at very low moisture content and moderate temperatures, *Transp. Porous Med.* 41 (2) (2000) 137–147.
- [18] B. Usovicz, Statistical-physical model of thermal conductivity in soil, *Polish J. Soil Sci.* XXV/1 (1992) 27–34.
- [19] R. Walczak, B. Usovicz, Variability of moisture, temperature and thermal properties in bare soil and in crop field, *Int. Agrophys.* 8 (1994) 161–169.
- [20] A. Gumuzzio, L. Brocca, N. Sánchez, A. González-Zamora, J. Martínez-Fernández, Comparison of SMOS, modelled and in situ long-term soil moisture series in the northwest of Spain, *Hydrol. Sci. J.* 61 (14) (2016).
- [21] S. Peischl, J.P. Walker, D. Ryu, Y.H. Kerr, R. Panciera, C. Rüdiger, Wheat canopy structure and surface roughness effects on multiangle observations at L-band, *IEEE Trans. Geosci. Remote Sens.* 50 (2012) 1498–1506.
- [22] K. Saleh, J. Wigneron, J. Calvet, E. Lopez-Baeza, P. Ferrazzoli, M. Berger, et al., The eurostars airborne campaign in support of the SMOS mission: first results over land surfaces, *Int. J. Remote Sens.* 25 (2004) 177–194.
- [23] A. Wilczek, A. Szyplowska, M. Kafarski, W. Skierucha, A time-domain reflectometry method with variable needle pulse width for measuring the dielectric properties of materials, *Sensors (Basel)* 16 (2) (2016) 191, <http://dx.doi.org/10.3390/s16020191>.
- [24] M.A. Shirazi, L. Boersma, C. Burch Johnson, Particle-size distributions: comparing texture systems, adding rock, and predicting soil properties, *Soil Sci. Soc. Am. J.* 65 (2) (2001) 300–310, <http://dx.doi.org/10.2136/sssaj2001.652300x>.
- [25] B. Usovicz, Evaluation of methods for soil thermal conductivity calculations, *Int. Agrophys.* 9 (2) (1995) 109–113.
- [26] S. Peischl, J.P. Walker, C. Rüdiger, N. Ye, Y.H. Kerr, E. Kim, R. Bandara, M. Allahmoradi, The AACES field experiments: SMOS calibration and validation across the Murrumbidgee River catchment, *Hydrol. Earth Syst. Sci.* 16 (2012) 1697–1708, <http://dx.doi.org/10.5194/hess-16-1697-2012>.
- [27] O. Merlin, J.P. Walker, R. Panciera, R. Young, J.D. Kalma, E.J. Kim, Soil moisture measurement in heterogeneous terrain, *Proc. MODSIM (2007)* 2604–2610.
- [28] M. Ryzak, A. Bieganski, Determination of particle size distribution of soil using laser diffraction – comparison with areometric method, *Int. Agrophys.* 24 (2010) 177–181.
- [29] F. James, *Statistical Methods in Experimental Physics*, 2nd ed., World Scientific, 2006.
- [30] B. Usovicz, L.B. Usovicz, ThermalWin beta (Soil thermal properties software package), Institute of Agrophysics, Polish Academy of Sciences, Lublin, 2004, Copyright 2004.
- [31] K.M. Smits, A. Cihan, T. Sakaki, T.H. Illangasekare, Evaporation from soils under thermal boundary conditions: experimental and modeling investigation to compare equilibrium-and nonequilibrium-based approaches, *Water Resour. Res.* 47 (5) (2011).
- [32] I. Samuel, S. Haruna, N. Nkongolo, Variability of soil physical properties in a clay-loam soil and its implication on soil management practices, *ISRN Soil Sci.* 2013 (2013), <http://dx.doi.org/10.1155/2013/418586>.
- [33] R. Webster, M. Oliver, *Statistical methods in soil and land resource survey*, Oxford University Press, NY, 1990, pp. 1–316.
- [34] A. Verhoef, Bart J.J.M. van den Hurk, Adrie F.G. Jacobs, Bert G. Heusinkveld, Thermal soil properties for vineyard (EFEDA-I) and savanna (HAPEX-Sahel) sites, *Agric. Forest Meteorol.* 78 (1–2) (1996) 1–18.
- [35] Database Tutiempo.net <http://en.tutiempo.net/climate/australia.html>.
- [36] A.I.J.M. van Dijk, H.E. Beck, R.S. Crosbie, R.A.M. de Jeu, Y.Y. Liu, G.M. Podger, B. Timbal, N.R. Viney, The Millennium Drought in southeast Australia (2001–2009): Natural and human causes and implications for water resources, ecosystems, economy, and society, *Water Resour. Res.* 49 (2013), <http://dx.doi.org/10.1002/wrcr.20123>.
- [37] B. Usovicz, J. Kossowski, P. Baranowski, Spatial variability of soil thermal properties in cultivated fields, *Soil Tillage Res.* 39 (1996) 85–100.
- [38] Google Earth software V 7.1.8.3036, Australia. 35°00'S 146°30'W, eye alt. 638 km. Image Landsat, Data SIO, NOAA, U.S. Navy, NGA, GEBCO, Google 2016.